# VLBI imaging of extremely high redshift quasars at 5 GHz

Paragi, Z.; Frey, S.; Gurvits, L.I.; Kellermann, K.I.; Schilizzi, R.T.; McMahon, R.G.; ... ; Pauliny-Toth, I.I.K.

Astron. Astrophys. 344, 51–60 (1999)

ASTRONOMY AND ASTROPHYSICS

# VLBI imaging of extremely high redshift quasars at 5 GHz

**Z. Paragi[1,2], S. Frey[1], L.I. Gurvits[2,3], K.I. Kellermann[4], R.T. Schilizzi[2,5], R.G. McMahon[6], I.M. Hook[7], and I.I.K. Pauliny-Toth[8]**

[1] FÖMI Satellite Geodetic Observatory, P.O. Box 546, H-1373 Budapest, Hungary
[2] Joint Institute for VLBI in Europe, P.O. Box 2, 7990 AA, Dwingeloo, The Netherlands
[3] Astro Space Center of P.N. Lebedev Physical Institute, 117924 Moscow, Russia
[4] National Radio Astronomy Observatory, 520 Edgemont Road, Charlottesville, VA 22903-2475, USA
[5] Leiden Observatory, P.O. Box 9513, 2300 RA, Leiden, The Netherlands
[6] Institute of Astronomy, Madingley Road, Cambridge CB3 0HA, UK
[7] European Southern Observatory, D-85748 Garching, Germany
[8] Max-Planck-Institut für Radioastronomie, Auf dem Hügel 69, D-53121 Bonn, Germany

Received 13 November 1998 / Accepted 8 January 1999

**Abstract.** We present very long baseline interferometry (VLBI) images of ten very high redshift ($z > 3$) quasars at 5 GHz. The sources 0004+139, 0830+101, 0906+041, 0938+119 and 1500+045 were observed in September 1992 using a global VLBI array, while 0046+063, 0243+181, 1338+381, 1428+423 and 1557+032 were observed in October 1996 with the European VLBI Network and Hartebeesthoek, South Africa. Most of the sources are resolved and show asymmetric structure. The sample includes 1428+423, the most distant radio loud quasar known to date ($z = 4.72$). It is barely resolved with an angular resolution of about 2.0×1.4 mas.

**Key words:** galaxies: quasars: general – radio continuum: galaxies – galaxies: active

## 1. Introduction

There are about fifty known radio loud quasars at redshift $z > 3$ with a total flux density at 5 GHz $S_5 \gtrsim 100$ mJy. Some of them have been imaged at 5 GHz with VLBI (Gurvits et al. 1992, 1994; Xu et al. 1995; Taylor et al. 1994; Frey et al. 1997; Udomprasert et al. 1997). Here we present first epoch VLBI images of a further ten $z > 3$ quasars. We show that their structural properties are similar to those of other known sources at $z > 3$. The present sample includes the most distant radio loud quasar known to date, 1428+423 at $z = 4.72$ (Hook & McMahon 1998).

Our interest in studying the milliarcsecond radio structures in high redshift quasars is motivated in part by their potential usefulness for cosmological tests (e.g. Kellermann 1993; Gurvits et al. 1999). Recent analysis of a sample of 151 quasars imaged at 5 GHz with milliarcsecond resolution has led to the conclusion that a simple assumption about the spectral properties of "cores" and "jets" can explain the apparent greater compactness of the sources at higher redshift (Frey et al. 1997; Gurvits et al. 1999). However, this result is based on a sample with considerable spread of structural properties on milliarcsecond scale. More data on the milliarcsecond radio structures, especially at high redshift are needed to study the structural properties of the quasars as well as various cosmological models to test.

*Send offprint requests to*: Z. Paragi, 1st address (paragi@sgo.fomi.hu)

## 2. Observations, calibration and data reduction

Five sources (0004+139, 0830+101, 0906+041, 0938+119 and 1500+045) were observed during a single 24 hour observing run using a global VLBI array on 27/28 September 1992. Another five sources (0046+063, 0243+181, 1338+381, 1428+423 and 1557+032) were observed with the European VLBI Network (EVN) and the Hartebeesthoek Radio Astronomical Observatory 26 m antenna in South Africa on 25/26 and 27/28 October 1996. Source coordinates, redshifts and total flux densities at 6 cm are given in Table 1. The parameters of the radio telescopes used in the two experiments are shown in Table 2. The observations were made at 5 GHz in left circular polarization. Data were recorded using the Mk III VLBI system in Mode B with 28 MHz total bandwidth, and correlated at the MPIfR correlator in Bonn, Germany.

Initial calibration was done using the NRAO AIPS package (Cotton 1995; Diamond 1995). Clock offset and instrumental delay errors were corrected using the strong sources 0804+499 and 0235+164 in the global and the EVN experiments, respectively. Data were fringe-fitted using AIPS using 5 minute solution intervals. We used the system temperatures measured during the observations and previously determined gain curves for each telescope for the initial amplitude calibration, which was then adjusted using amplitude calibrator sources, based on total flux density values measured nearly contemporaneously to our observations with the Effelsberg telescope. For the September 1992 experiment, this was also checked using VLA data obtained in parallel with our VLBI observation. Total flux densities

**Table 1.** Source parameters

| Source | RA (J2000) (h) | (m) | (s) | Dec (J2000) (°) | (′) | (″) | $S^{a}$ (mJy) | $z$ |
|---|---|---|---|---|---|---|---|---|
| 0004+139 | 00 | 06 | 57.536 | 14 | 15 | 46.750 | $152 \pm 14$ | 3.25[b] |
| 0046+063 | 00 | 48 | 58.740 | 06 | 40 | 05.900 | $211 \pm 19$ | 3.52[b] |
| 0243+181 | 02 | 46 | 11.830 | 18 | 23 | 30.200 | $220 \pm 20$ | 3.59[b] |
| 0830+101 | 08 | 33 | 22.514 | 09 | 59 | 41.140 | $93 \pm 9$ | 3.75[c] |
| 0906+041 | 09 | 09 | 15.915 | 03 | 54 | 42.980 | $111 \pm 11$ | 3.20[d] |
| 0938+119 | 09 | 41 | 13.562 | 11 | 45 | 36.210 | $123 \pm 12$ | 3.177[e] |
| 1338+381 | 13 | 40 | 22.952 | 37 | 54 | 43.833 | $211 \pm 23$ | 3.10[f] |
| 1428+423 | 14 | 30 | 23.742 | 42 | 04 | 36.503 | $337 \pm 30$ | 4.72[g] |
| 1500+045 | 15 | 03 | 28.886 | 04 | 19 | 48.980 | $147 \pm 14$ | 3.67[h] |
| 1557+032 | 15 | 59 | 30.973 | 03 | 04 | 48.257 | $414 \pm 37$ | 3.90[h] |

[a] total flux density at 5 GHz from Gregory et al. 1996
[b] Hook 1994; Hook & McMahon (in prep.)
[c] Oren & Wolfe 1995
[d] Brinkmann et al. 1997
[e] Osmer et al. 1994
[f] Hook et al. 1995
[g] Hook & McMahon 1998
[h] McMahon et al. 1994

**Table 2.** VLBI telescopes in the September 1992 (top) and October 1996 experiment (bottom) and their characteristics at 5 GHz

| Radio telescope | Diameter (m) | SEFD[a] (Jy) |
|---|---|---|
| Effelsberg | 100 | 20 |
| Medicina | 32 | 296 |
| Onsala | 25 | 780 |
| Westerbork | 93[b] | 108 |
| NRAO Green Bank | 43 | 77 |
| Haystack | 37 | 533 |
| VLBA Owens Valley | 25 | 289 |
| VLA | 115[b] | 5.3 |
| Effelsberg | 100 | 20 |
| Jodrell Bank Mk2 | 26 | 320 |
| Noto | 32 | 260 |
| Torun | 32 | 220 |
| Simeiz | 22 | 3000 |
| Sheshan | 25 | 520 |
| Nanshan | 25 | 350 |
| Hartebeesthoek | 26 | 790 |

[a] System Equivalent Flux Density
[b] The telescope was used in phased array mode; an equivalent diameter is given.

determined from VLBI images were typically 10–15% smaller than those determined from the VLA observations, which may indicate either the presence of extended structures undetectable with VLBI or residual calibration errors.

The Caltech DIFMAP program (Shepherd et al. 1994) was used for self–calibration and imaging, starting with point source models with flux densities consistent with the zero–spacing values. RMS image noises (3 $\sigma$) were 0.2–0.4 and 0.6–1.0 mJy/beam (depending on the telescopes' performance and integrated on–source time) for the global and the EVN experiments, respectively. Plots of self–calibrated correlated flux densities as a function of projected baseline length, as well as clean images resulting from the DIFMAP imaging process are shown in Fig. 1 for both experiments. Image parameters are listed in Table 3. All sources but the most distant one, 1428+423, appear to be well resolved and most of them show asymmetric structure.

We performed model fitting in DIFMAP using self–calibrated $uv$-data in order to quantitatively compare these sources with other extremely high redshift quasars. The results of model fitting are listed in Table 4. In all cases we fixed the first component at the phase center. While we searched for the simplest possible model (i.e. the smallest possible number of Gaussian components), not all components can be distinguished as separate features on the maps. In the case of 0004+139, we kept only one component for the extended emission because the position angle of the beam lies close to the source structure direction and the correlated flux density versus $uv$–distance plot indicates the presence of a large component.

We also made $14''$ resolution VLA D configuration images of the five sources observed in the 1992 global experiment. VLA data were obtained at the same time as the phased array data used for the global VLBI experiment. These images were made using the NRAO AIPS package with typically 3–6 iterations of self–calibration and imaging. We show VLA images of 0830+101 and 1500+045 in Fig. 2a and 2b, respectively. The other three sources appeared unresolved with the VLA in our observations.

## 3. Comments on individual sources

*0004+139* The spectral indices of the source ($S \propto \nu^{\alpha}$ throughout this paper) are $\alpha_{0.365}^{1.4} = -0.6$ and $\alpha_{1.4}^{4.85} = -0.4$ (White & Becker 1992). It is unresolved with the VLA A-array ($\sim 400$ mas resolution) at 5 GHz (Lawrence et al. 1986).

Our VLBI image shows structure extending up to about 10 mas from the core to the SE direction (Fig. 1a). The position angle of the beam is not well suited to resolve the fine details of this jet–like extension. The source is unresolved with the VLA D-array in our experiment with $14''$ resolution.

*0046+063* The source has a flat radio spectrum between 1.4 and 4.85 GHz ($\alpha_{1.4}^{4.85} = -0.0$, White & Becker 1992). Our VLBI image shows a dominant central component and a prominent secondary component separated by 3.8 mas from the core in the NE direction (Fig. 1b).

*0243+181* The spectral index of this quasar is $\alpha_{1.4}^{4.85} = 0.1$ (White & Becker 1992). Apart from the compact core, there is a weak extended feature 4.9 mas to the South (Fig. 1c).

*0830+101* The source is reported to be unresolved at 5 GHz with the VLA B–array ($\sim 1.2''$ resolution), no extended emission has been found within about $51''$ from the core (Lawrence

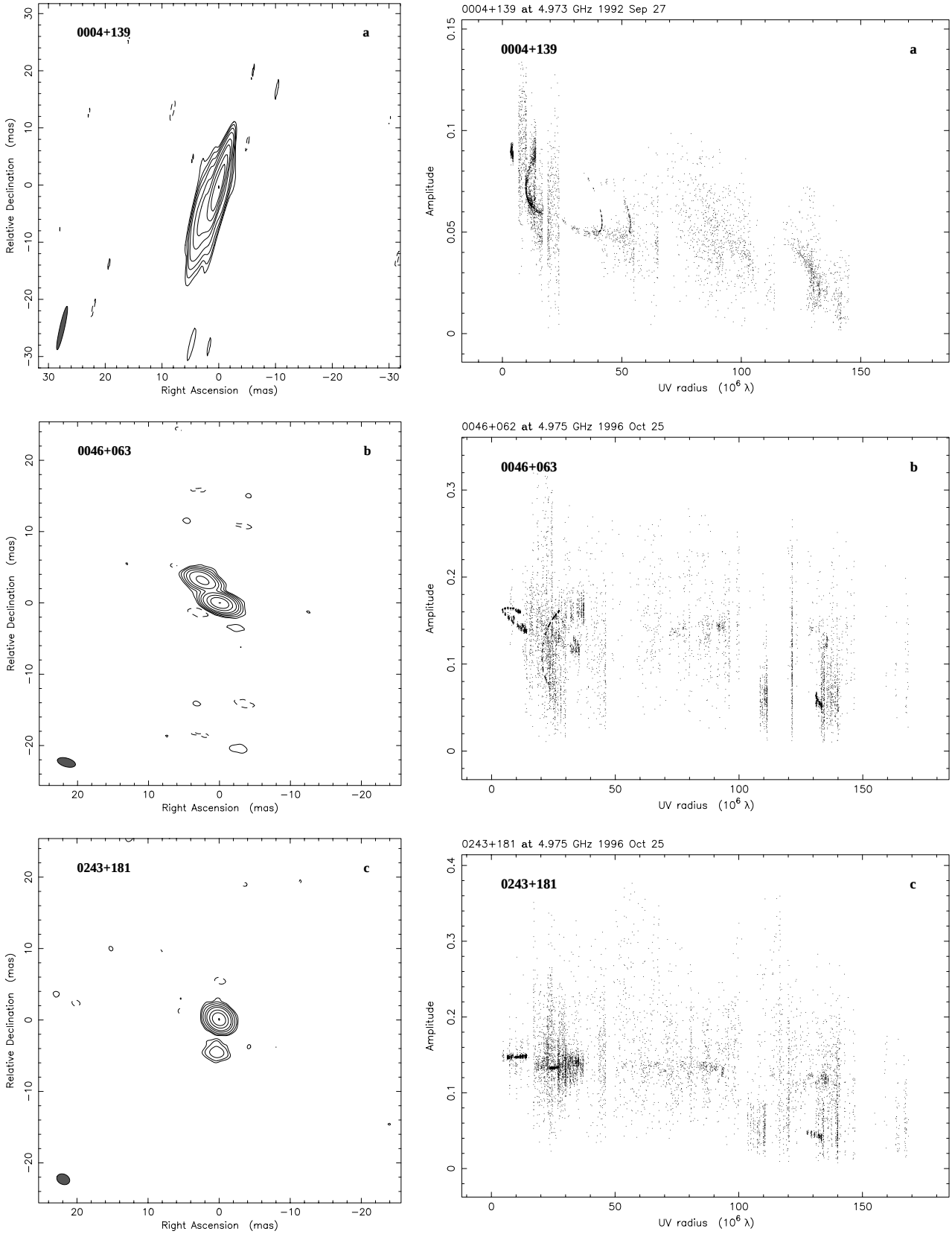


**Fig. 1a–j.** "Naturally" weighted 5 GHz images (*left*) and correlated flux density (Jy) versus projected baseline length (*right*) for **a** 0004+139, **b** 0046+063, **c** 0243+181, **d** 0830+101, **e** 0906+041, **f** 0938+119, **g** 1338+381, **h** 1428+423, **i** 1500+045 and **j** 1557+032. Map parameters are given in Table 3

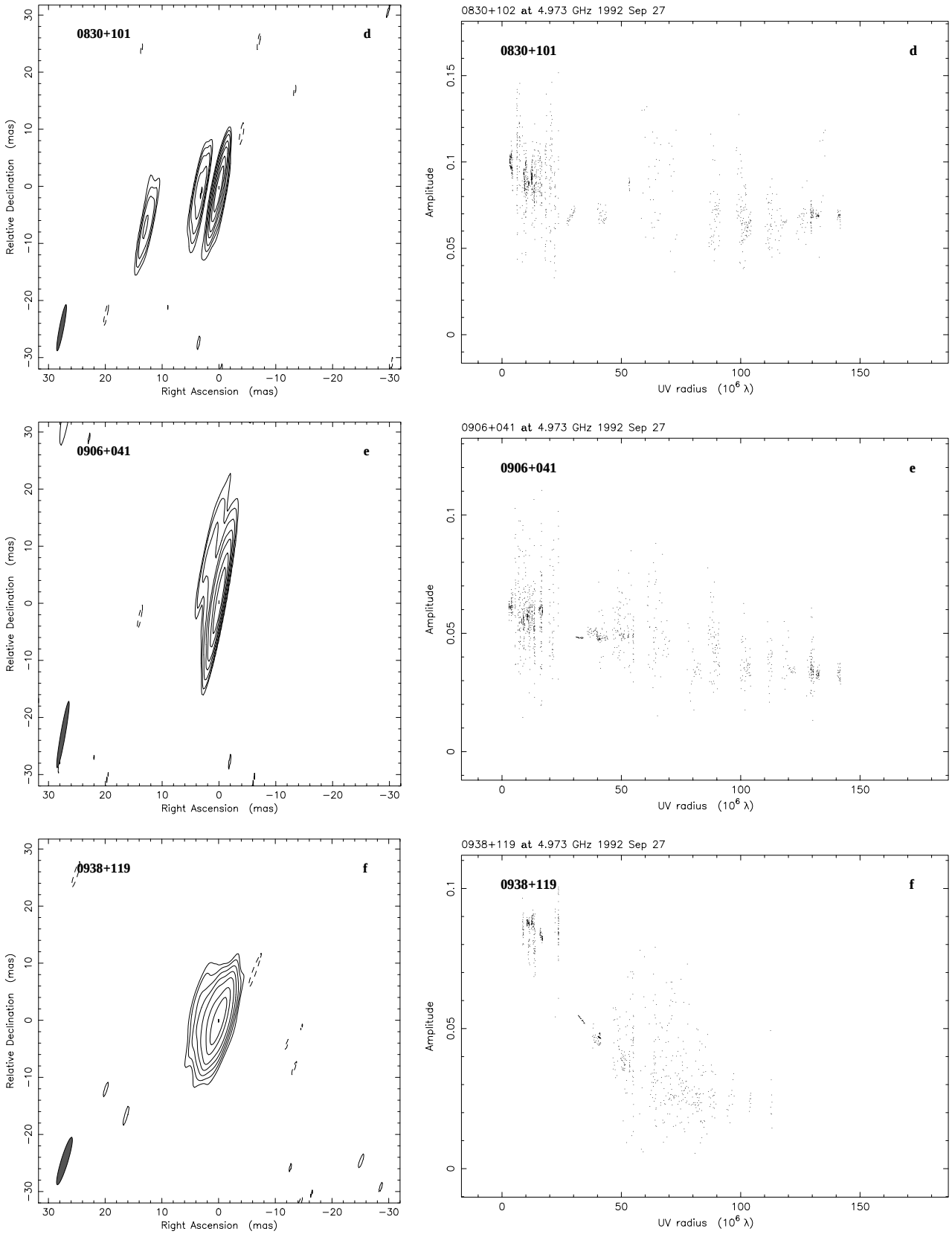


**Fig. 1a–j.** (continued)

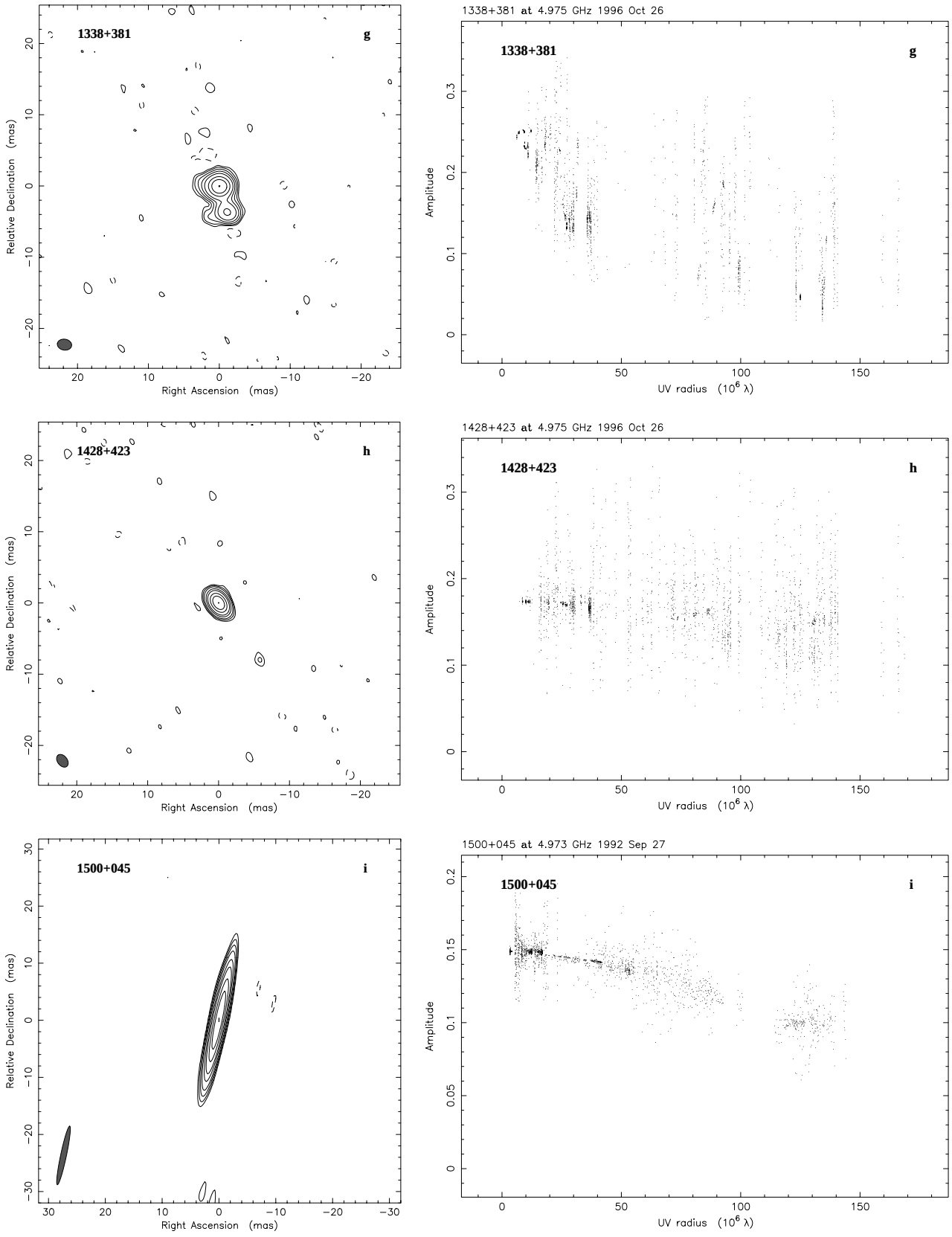


**Fig. 1a–j.** (continued)

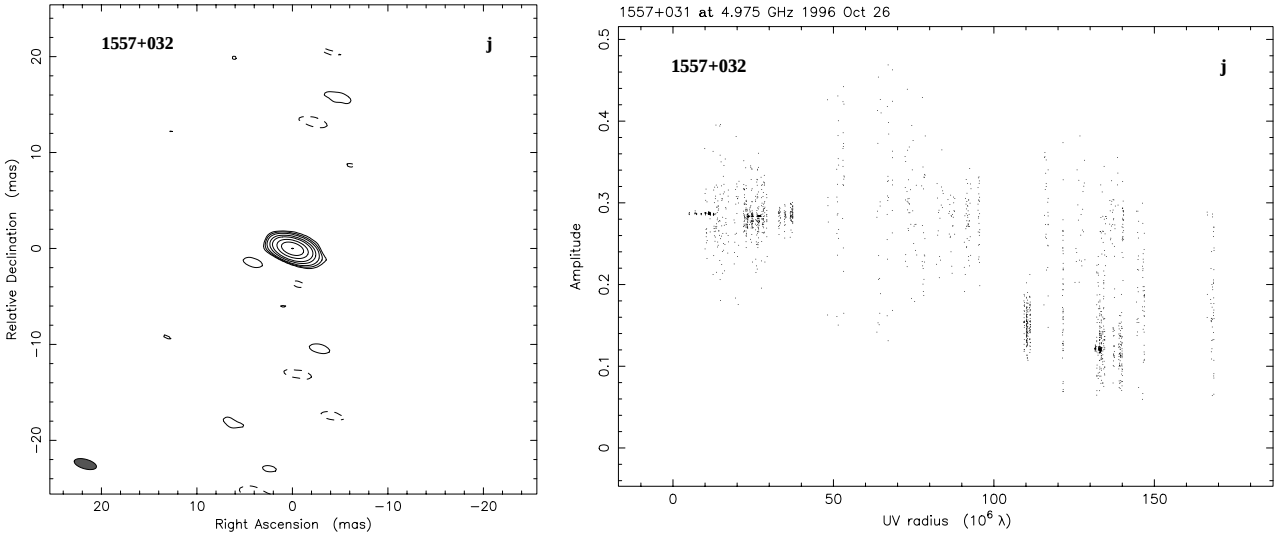


**Fig. 1a–j.** (continued)

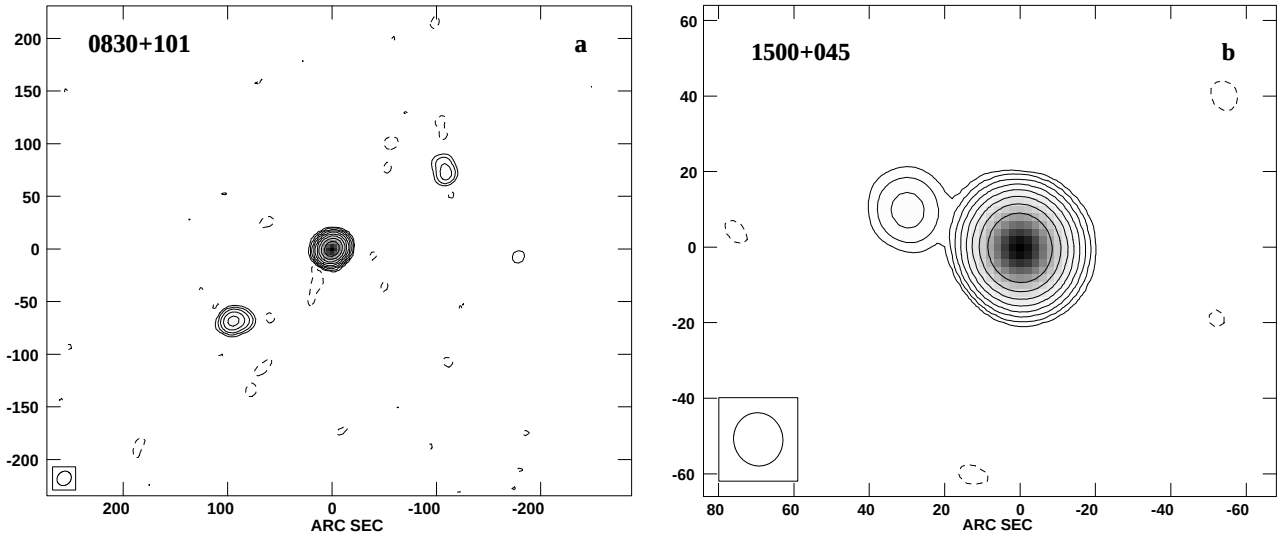


**Fig. 2a and b.** 5 GHz VLA images of **a** 0830+101 and **b** 1500+045. The contour levels are **a** $-1$, 1, 2, 4, 8, 16, 32, 64, 128, 256, 512, 1024 $\times$ 0.1 mJy/beam and **b** $-1$, 1, 2, 4, 8, 16, 32, 64, 128, 256 $\times$ 0.2 mJy/beam. The restoring circular beam is $14''$ (HPBW)

**Table 3.** Parameters of VLBI maps in Fig. 1a-j

| Source | Contour levels | Peak brightness | Restoring beam | | | Observing epoch |
|---|---|---|---|---|---|---|
| | | | $\theta_{max}$ | $\theta_{min}$ | PA | |
| | (% of the peak brightness) | (mJy/beam) | (mas) | (mas) | ($^\circ$) | |
| 0004+139 | $-0.25$, 0.25, 0.5, 1, 2, 5, 10, 25, 50, 99 | 50 | 7.8 | 0.8 | $-13$ | Sep 1992 |
| 0046+063 | $-0.6$, 0.6, 1.2, 2.5, 5, 10, 25, 50, 99 | 104 | 2.6 | 1.2 | 74 | Oct 1996 |
| 0243+181 | $-0.4$, 0.4, 0.8, 2, 5, 10, 25, 50, 99 | 119 | 1.9 | 1.4 | 66 | Oct 1996 |
| 0830+101 | $-0.5$, 0.5, 1, 2, 5, 10, 25, 50, 99 | 74 | 8.2 | 0.8 | $-11$ | Sep 1992 |
| 0906+041 | $-0.4$, 0.4, 0.8, 2, 5, 10, 25, 50, 99 | 44 | 11.8 | 0.8 | $-10$ | Sep 1992 |
| 0938+119 | $-0.6$, 0.6, 1.2, 2.5, 5, 10, 25, 50, 99 | 49 | 8.7 | 1.2 | $-17$ | Sep 1992 |
| 1338+381 | $-0.6$, 0.6, 1.2, 2.5, 5, 10, 25, 50, 99 | 148 | 2.0 | 1.5 | 81 | Oct 1996 |
| 1428+423 | $-0.5$, 0.5, 1, 2, 5, 10, 25, 50, 99 | 161 | 2.0 | 1.4 | 38 | Oct 1996 |
| 1500+045 | $-0.25$, 0.25, 0.5, 1, 2, 5, 10, 25, 50, 99 | 131 | 10.5 | 1.0 | $-12$ | Sep 1992 |
| 1557+032 | $-0.5$, 0.5, 1, 2, 5, 10, 25, 50, 99 | 228 | 2.4 | 1.0 | 75 | Oct 1996 |

*Note:* $\theta_{max}$, $\theta_{min}$ and PA are restoring beam major axis, minor axis and position angle, respectively.

et al. 1986). The spectral index of the source is $\alpha_{1.4}^{4.85} = -0.3$ (White & Becker 1992). On the VLBI scale, it has two bright components near the core that perhaps delineate a slightly curved jet extending up to ∼15 mas (Fig. 1d). Our VLA D-array map shows two faint components about $2'$ from the core to the SE and NW which resembles a classical double lobe structure (Fig. 2a). However, it is not clear from our VLA image whether these sources are physically related to 0830+101 or they are chance coincidences. The latter seems to be unlikely, but could not be ruled out based on our data.

*0906+041* Spectral indices of $\alpha_{0.365}^{1.4} = 0.1$ and $\alpha_{1.4}^{4.85} = -0.4$ are given by White & Becker (1992). If the flux density of the source did not change between the epochs of measurements this indicates that the source may be a Gigahertz Peaked Spectrum (GPS) quasar. This object has been identified as a ROSAT X–ray source (RXJ0909.2+0354). Its flux in the 0.1–2.4 keV range is $f_x = 9.9 \pm 2.7\ 10^{-13}$ erg cm$^{-2}$ s$^{-1}$ (Brinkmann et al. 1995). The source is unresolved with the VLA D-array at 5 GHz. On VLBI scales, the core of 0906+041 is resolved with an extension to the NE (Fig. 1e). A secondary compact component is separated by about 10 mas from the core.

*0938+119* This source is identified as a quasar by Beaver et al. (1976) and has a very steep optical continuum more typical of BL Lac objects (Baldwin et al. 1976). The radio continuum peaks near 1 GHz ($\alpha_{0.365}^{1.4} = -0.0$ and $\alpha_{1.4}^{4.85} = -0.7$, White & Becker 1992). Neff & Hutchings (1990) found radio emission with the VLA at 1.4 GHz on both sides of the radio core extending to $5''$ and $2''$ from the centre. The source was studied in high energy bands, however, only upper limits are available for X–ray and $\gamma$–ray luminosities (Zamorani et al. 1981; Fichtel et al. 1994). The source is resolved by our observations and shows an extension of about 5 mas to the East (Fig. 1f). It is unresolved with the VLA in our experiment.

*1338+381* This flat spectrum source ($\alpha_{1.4}^{4.85} = -0.0$, White & Becker 1992) is a candidate IERS radio reference frame object and serves as a link to the HIPPARCOS stellar reference frame (Ma et al. 1997). It is being monitored by geodetic VLBI networks at 2.3 and 8.4 GHz. In our 5 GHz imaging experiment the source appears to be resolved and shows a double structure elongated in the S-SW direction with the angular separation of 3.65 mas (Fig. 1g). The component position angle and separation are in very good agreement with a recent 8.4 GHz global VLBI image by Bouchy et al. (1998). Due to the lower resolution of our image we can not decide whether their component "c" is present between the two dominant components seen in our image.

*1428+423* The radio spectral indices of the quasar 1428+423 – also known as GB1428+4217 (Fabian et al. 1997; Hook & McMahon 1998) and B3 1428+422 (Véron-Cetty & Véron 1998) – are $\alpha_{0.365}^{1.4} = 0.5$ and $\alpha_{1.4}^{4.85} = -0.4$ (White & Becker 1992) which are typical for GPS sources. It is the third highest redshift quasar known to date (Hook & McMahon 1998, $z = 4.72$) and the most distant known radio loud quasar. The quasar was detected in X-rays with the ROSAT High Resolution Imager in the (observed) 0.1–2.4 keV band (Fabian et al. 1997) and with various ASCA detectors in the (observed) band of 0.5–10 keV (Fabian et al. 1998). Both observations are in agreement and indicate that the SED of this source is strongly dominated by X- and $\gamma$-ray emission. The X-ray spectrum is remarkably flat. The quasar might be the most luminous steady source in the Universe, with an apparent luminosity in excess of $10^{47}$ erg s$^{-1}$. The extreme X-ray luminosity of the quasar 1428+423 suggests that the emission is highly beamed toward us (Fabian et al. 1997, 1998).

Our VLBI image (Fig. 1h) is in qualitative agreement with the relativistic beaming model of the source. The quasar appears to be almost unresolved with the VLA at 5 GHz (Laurent-Muehleisen et al. 1997) as well as by our VLBI observations up to 170 M$\lambda$, which corresponds to an angular resolution of 2.0×1.4 mas. The other two $z > 4$ quasars imaged with VLBI also appear unresolved (1251−407 and 1508+572, Frey et al. 1997), which suggests that the high $z$ quasars may be systematically more compact then their less distant counterparts. Alternatively, as suggested by Fabian et al. (1997), the highly beamed emission might be responsible for a selection effect resulting in detection of an otherwise weaker population of extremely high redshift quasars.

*1500+045* This source was detected as a $5 \pm 2.4$ mJy source at 240 GHz by McMahon et al. (1994) corresponding to $\alpha_5^{240} = -0.9$. The spectral index between 1.4 and 4.85 GHz is $\alpha_{1.4}^{4.85} = 0.2$ (White & Becker 1992). The source is unresolved with the VLA B–array (∼ $1.2''$ resolution, Lawrence et al. 1986).

Although the source is resolved, our VLBI image does not show any structure (Fig. 1i). Our VLA image shows an extension to E-NE at about $33''$ (Fig. 2b).

*1557+032* This quasar is an IERS Celestial Reference Frame candidate source (Ma et al. 1997). It was also detected with the Parkes–Tidbinbilla interferometer at 2.3 GHz (Duncan et al. 1993) and found to be compact with a total flux density of 376 mJy. Our VLBI observations show that the source is resolved but featureless (Fig. 1j). There is no extended feature found down to 0.5% of the peak brightness.

## 4. Discussion

Frey et al. (1997) studied the parsec scale structural properties of radio loud QSO's using a sample of 151 quasars in the redshift range of $0.2 < z < 4.5$ observed with sufficiently high resolution at 5 GHz. They determined the flux density ratios of the brightest "jet" and "core" components ($S_j/S_c$) of the sources. The typical angular resolution of those VLBI observations was ∼1 mas. Because the linear resolution is better for the lowest redshift sources, they introduced a linear size limit to distin-

**Table 4.** Fitted elliptical Gaussian model parameters of the source structures

| Source | Component | $S$ (mJy) [1] | $r$ (mas) [2] | $\Theta$ (°) [3] | $a$ (mas) [4] | $b/a$ [5] | $\Phi$ (°) [6] | Agreement factor [7] | $S_j/S_c$ [8] |
|---|---|---|---|---|---|---|---|---|---|
| 0004+139 | A | 56 | 0.0 | – | 2.5 | 0.0 | −32 | 0.94 | – |
| | B | 37 | 4.0 | 156 | 5.8 | 3.6 | −28 | | |
| 0046+063 | A | 117 | 0.0 | – | 0.7 | 0.3 | 17 | 1.06 | 0.40 |
| | B | 47 | 3.8 | 37 | 1.5 | 0.1 | 36 | | |
| 0243+181 | A | 96 | 0.0 | – | 0.8 | 0.6 | 3 | 1.03 | 0.05 |
| | B | 48 | 0.4 | 5 | 1.5 | 0.0 | 1 | | |
| | C | 5 | 4.9 | 176 | 0.8 | 0.7 | 59 | | |
| 0830+102 | A | 81 | 0.0 | – | 1.2 | 0.3 | 0 | 0.99 | 0.22 |
| | B | 18 | 4.0 | 120 | 2.8 | 0.0 | −33 | | |
| | C | 7 | 15.8 | 123 | 4.7 | 0.0 | −26 | | |
| 0906+041 | A | 35 | 0.0 | – | 2.5 | 0.1 | −10 | 0.90 | 0.63 |
| | B | 22 | 2.1 | 4 | 1.5 | 0.0 | −70 | | |
| | C | 2 | 9.3 | 8 | 5.8 | 0.1 | −13 | | |
| 0938+119 | A | 50 | 0.0 | – | 1.2 | 0.1 | 55 | 0.85 | <0.005 |
| | B | 40 | 0.6 | 106 | 4.1 | 0.3 | 51 | | |
| 1338+381 | A | 187 | 0.0 | – | 1.1 | 0.6 | −10 | 1.04 | 0.32 |
| | B | 10 | 1.6 | 116 | 3.7 | 0.2 | −80 | | |
| | C | 60 | 3.7 | −163 | 1.2 | 0.3 | 13 | | |
| 1428+423 | A | 173 | 0.0 | – | 0.6 | 0.5 | 11 | 0.95 | <0.005 |
| 1500+045 | A | 138 | 0.0 | – | 0.7 | 0.0 | 28 | 0.95 | – |
| | B | 11 | 0.7 | 97 | 3.3 | 0.2 | −11 | | |
| 1557+032 | A | 276 | 0.0 | – | 0.7 | 0.0 | 2 | 1.11 | 0.05 |
| | B | 15 | 1.1 | −154 | 4.6 | 0.0 | 76 | | |

[1] $S$ flux density,
[2] $r$ angular separation from the central component,
[3] $\Theta$ position angle (Position angles are measured from the North through East),
[4] $a$ component major axes,
[5] $b/a$ ratio of the component minor and major axes,
[6] $\Phi$ component major axis position angle,
[7] The agreement factor is the square root of reduced $\chi^2$, see e.g. Pearson (1995),
[8] $S_j/S_c$ jet to core flux density ratio.

guish between jet and core components in order to compare the same linear sizes at different redshifts. One milliarcsecond sets the linear resolution to 7 pc for $z \gtrsim 1$ sources up to the highest redshifts represented in the sample ($H_0$=80 km s$^{-1}$ Mpc$^{-1}$ and $q_0$=0.1 were used to calculate linear sizes; the angular size of a fixed linear size is practically constant at $z \gtrsim 1$ for plausible cosmological models). The value of 7 pc was not used in any quantitative way in their analysis, just as a threshold between cores and jets. Only components outside the core region were considered as jet components. They found a weak overall trend of a decreasing jet to core flux density ratio with increasing redshift which may be explained by the combined effect of the shifts of the emitting frequencies at different redshifts compared to the 5 GHz observing frequency and the different characteristic spectral indices in cores and jets.

We followed Frey et al. (1997) and calculated the jet to core flux density ratios ($S_j/S_c$) for the $z > 3$ sources presented in this paper (last column of Table 4). We had to exclude two sources from the analysis, 0004+139 and 1500+045. In the former case, the angular resolution in the direction of the expected jet structure is considerably greater than 1 mas. The quasar 1500+045 may also have jet structure which is not observable in our data due to the unfortunate orientation of the 10.5 mas restoring beam. The $S_j/S_c$ values for the other three sources observed in the 1992 global experiment (0830+101, 0906+041 and 0938+119) should also be interpreted with caution since the restoring beam is very elongated. However, we derived tentative $S_j/S_c$ values because the direction of the jet structure indicated by our maps are nearly perpendicular to the major axis of the beam and the resolution in this direction is about 1 mas. In the case of 0938+119 and 1428+423, an upper limit of the jet flux density was calculated based on the beam sizes and the 3$\sigma$ RMS noises on our images.

We added our eight new sources to the sample of Frey et al. (1997). The median $S_j/S_c$ values as function of redshift are shown in Fig. 3. The data for all 159 sources are evenly

grouped into 13 bins. Error bars indicate the mean absolute deviation of data points from the median within each bin. Upper limits and measured values are treated similarly. However, the plotted error bars are indicative of the scatter of the data. The solid curve represents the best least squares fit based on the 13 median values. Under the assumption that intrinsic spectral properties at the sources could be described by simple power–law dependence, the average difference between jet and core spectral indices can be estimated as $\alpha_j - \alpha_c = -0.62 \pm 0.45$.

The three circles at the high redshift end of the plot in Fig. 3 show the upper limits of the jet to core flux density ratios for the most distant ($z > 4$) quasars imaged at 5 GHz with VLBI to date. The sources 1251−407 ($z = 4.46$, Shaver et al. 1996) and 1428+423 ($z = 4.72$, Hook & McMahon 1998) are represented by filled circles. The open circle corresponds to the quasar 1508+572 ($z = 4.30$, Hook et al. 1995) which also appeared to be unresolved, however, at a considerably lower angular resolution ($\sim 5$ mas) than the other sources included in the sample (Frey et al. 1997).

We note that in both cases available to date, radio structures in quasars at $z > 4$ (1251−407 and 1428+423) appear to be unresolved with a nominal resolution of ∼1 mas. The third case, 1508+572, albeit with a lower resolution of 5 mas, does not show a jet–like structure either. Qualitatively, it is consistent with the overall trend that steeper spectrum jets are fainter relative to flat spectrum cores at higher redshift because the fixed 5 GHz observing frequency implies high rest–frame frequency (for $z > 4$ the emitted frequency $\nu_{em} = \nu_{obs}(1+z) > 25$ GHz). However, these sources appear to be much more compact than expected from the general trend shown in Fig. 3. Even in the neighboring high redshift bins ($3 < z < 4$), it is unlikely that we find 3 randomly selected sources practically unresolved. A possible explanation for the observed compactness is that the spectral indices of the jet components become steeper with frequency, which results in a relative fading of the components with respect to the core at the high emitting frequencies (∼25 GHz) of the largest redshift sources. Future multi–frequency VLBI observations of more $z > 4$ radio loud quasars with the highest possible sensitivity and angular resolution should answer the question whether these objects are indeed intrinsically so compact or there is a strong observational selection effect responsible for their particularly compact appearance.

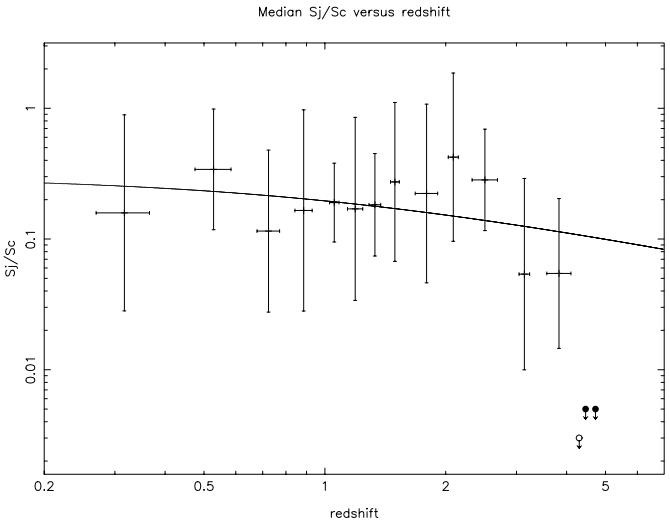


**Fig. 3.** Median jet to core flux density ratios versus redshift for 159 quasars of Frey et al. (1997) and this paper. Values are grouped into 13 nearly equally populated bins (12–13 sources per bin). The solid curve represents the best fit to the 13 median values. Circles indicate the upper limits of $S_j/S_c$ for the three $z > 4$ quasars imaged with VLBI at 5 GHz to date (see Sect. 4.)

## 5. Conclusion

We have presented 5 GHz VLBI images of ten extremely high redshift ($z > 3$) quasars including the most distant radio loud quasar known to date (1428+423, $z = 4.72$). Most of the sources are well resolved and their morphology is asymmetric. Based on fitted Gaussian source model components, we have determined the jet to core flux density ratios. The values obtained are typical of high redshift radio quasars for sources in the redshift range $3 < z < 4$. However, the most distant radio loud quasar, 1428+423, appears to be unusually compact.

*Acknowledgements.* We are grateful to the staff of the EVN, NRAO and Hartebeesthoek observatories, and the MPIfR correlator for their support of our project. We thank Joan Wrobel for assistance in preparation and analysis of the global VLBI experiment of 1992 described in the paper, and the referee for a number of very helpful suggestions. ZP and SF acknowledge financial support received from the European Union under contract CHGECT 920011, Netherlands Organization for Scientific Research (NWO) and the Hungarian Space Office, and hospitality of JIVE and NFRA during their fellowship in Dwingeloo. LIG acknowledges partial support from the EU under contract no. CHGECT 920011, the NWO programme on the Early Universe and the hospitality of the FÖMI Satellite Geodetic Observatory, Hungary (supported in part through the contract No. ERBCIPDCT940087 and by the Hungarian Space Office). LIG and RGM acknowledge partial support from the TMR Programme, Research Network Contract ERBFMRXCT 96–0034 “CERES”. The National Radio Astronomy Observatory is operated by Associated Universities, Inc. under a Cooperative Agreement with the National Science Foundation. This research has made use of the NASA/IPAC Extragalactic Data Base (NED) which is operated by the Jet Propulsion Laboratory, California Institute of Technology, under contract with the National Aeronautics and Space Administration.

## References

Baldwin J.A., Smith H.E., Burbidge E.M., et al., 1976, ApJ 206, L83
Beaver E.A., Harms A., Hazard C., et al., 1976, ApJ 203, L5
Bouchy F., Lestrade J.-F., Ransom R.R., et al., 1998, A&A 335, 145
Brinkmann W., Siebert J., Reich W., et al., 1995, A&AS 109, 147
Brinkmann W., Yuan W., Siebert J., 1997, A&A 319, 413
Cotton W.D., 1995, In: Zensus, J.A., Diamond, P.J., Napier, P.J. (eds.) Very Long Baseline Interferometry and the VLBA. ASP Conference Series 82, 189
Diamond P.J., 1995, In: Zensus, J.A., Diamond, P.J., Napier, P.J. (eds.) Very Long Baseline Interferometry and the VLBA. ASP Conference Series 82, 227
Duncan R.A., White G.L., Wark R., et al., 1993, Proc. Astron. Soc. Aust. 10, 310

Fabian A.C., Brandt W.N., McMahon R.G., Hook I.M., 1997, MNRAS 291, L5
Fabian A.C., Iwasawa K., Celotti A., et al., 1998, MNRAS 295, L25
Fichtel C.E., Bertsch D.L., Chiang J., et al., 1994, ApJS 94, 551
Frey S., Gurvits L.I., Kellermann K.I., Schilizzi R.T., Pauliny-Toth I.I.K., 1997, A&A 325, 511
Gregory P.C., Scott W.K., Douglas K., Condon J.J., 1996, ApJS 103, 427
Gurvits L.I., Kardashev N.S., Popov M.V., et al., 1992, A&A 260, 82
Gurvits L.I., Schilizzi R.T., Barthel P.D., et al., 1994, A&A 291, 737
Gurvits L.I., Kellermann K.I., Frey S., 1999, A&A, in press
Hook I.M., 1994, Ph.D. Thesis, University of Cambridge
Hook I.M., McMahon R.G., 1998, MNRAS 294, L7
Hook I.M., McMahon R.G., Patnaik A.R., et al., 1995, MNRAS 273, L63
Kellermann K.I. 1993, Nat 361, 134
Laurent-Muehleisen S.A., Kollgaard R.I., Ryan P.J., et al., 1997, A&AS 122, 235
Lawrence C.R., Bennett C.L., Hewitt J.N., et al., 1986, ApJS 61, 105
Ma C., Arias E.F., Eubanks T.M., et al., 1997, In: Ma C., Feissel M. (eds.) Definition and Realization of the International Celestial Reference System by VLBI Astrometry of Extragalactic Objects. IERS Technical Note 23, II–3
McMahon R.G., Omont A., Bergeron J., Kreysa E., Haslam C.G.T., 1994, MNRAS 267, L9
Neff S.G., Hutchings J.B., 1990, AJ 100, 1441
Oren A.L., Wolfe A.M., 1995, ApJ 445, 624
Osmer P.S., Porter A.C., Green R.F., 1994, ApJ 436, 678
Pearson T.J., 1995, In: Zensus, J.A., Diamond, P.J., Napier, P.J. (eds.) Very Long Baseline Interferometry and the VLBA. ASP Conference Series 82, 267
Shaver P.A., Wall J.V., Kellermann K.I., 1996, MNRAS 278, L11
Shepherd M.C., Pearson T.J., Taylor G.B., 1994, BAAS 26, 987
Taylor G.B., Vermeulen R.C., Pearson T.J., et al., 1994, ApJS 95, 345
Udomprasert P.S., Taylor G.B., Pearson T.J., Roberts D.H., 1997, ApJ 483, L9
Véron-Cetty M.-P., Véron P., 1998, A Catalogue of Quasars and Active Nuclei (8th Edition), ESA Sci. Rep. No. 18, Garching
White R.L., Becker R.H., 1992, ApJS 79, 331
Xu W., Readhead A.C.S., Pearson T.J., Polatidis A.G., Wilkinson P.N., 1995, ApJS 99, 297
Zamorani G., Henry J.P., Maccacaro T., et al., 1981, ApJ 245, 357